ELSEVIER

Cement & Concrete Composites 24 (2002) 159–167

Cement & Concrete Composites

www.elsevier.com/locate/cemconcomp

Protection current distribution in reinforced concrete cathodic protection systems

A.M. Hassanein, G.K. Glass *, N.R. Buenfeld

Department of Civil and Environmental Engineering, Imperial College, Imperial College Road, London SW7 2BU, UK

Abstract

Current distribution from a surface mounted anode to steel reinforcement in atmospherically exposed concrete is modelled as a function of the condition of the steel, the resistivity of the concrete and anode-steel geometry. The boundary conditions at the steel have a significant effect on current distribution with more uniform distribution arising at low steel corrosion rates. In a typical situation the surface of a steel bar facing the anode may receive 50% more current than the opposite surface. As cathodic protection has proved to be effective in these cases, a basis for many design decisions that influence current distribution is that their effect is small by comparison. When more than one layer of reinforcement is present the current distribution is significantly worse. In this case a surface anode may not be enough and discrete anodes may be necessary to improve current distribution. An increase in the concrete resistivity, cover and the anode to cathode area ratio at a constant anode current density will increase the voltage drop through the concrete inducing an improvement in the environment at the steel that promotes steel passivity. © 2002 Elsevier Science Ltd. All rights reserved.

Keywords: Cathodic protection; Chloride removal; Concrete; Reinforcement corrosion; Current distribution; Electric field; Electrochemical repair; Hydroxyl generation; Modelling

1. Introduction

One of the objectives in cathodic protection (CP) design is to deliver a fairly uniform current density to the protected steel. This will minimise the current required to achieve the protection criterion, thus reducing the cost and improving the life of the system components. The achievement of uniform current distribution in an atmospherically exposed reinforced concrete CP system is, however, hindered by the location of the steel in a resistive environment close to a large planar anode.

Much previous work [1–3] has examined current distribution with regard to the design of CP systems applied to steel elements/structures in sea water and soils using experimental methods and mathematical models. In mathematical models the boundary conditions at the polarising interfaces have always presented problems. In early works the resistance to polarisation presented by the interface was often ignored. Empirical functions approximating the polarisation behaviour have also been used and recent advances have allowed the time dependence of the polarisability of the cathodic interface resulting from the precipitation of deposits there to be modelled [4].

The distribution of current in reinforced concrete CP systems has been subject to less extensive analysis. Bertolini et al. [5] studied the screening effects of an outer steel bar on bars located at greater depths and modelled the experimental results using an empirical cathodic boundary condition. They noted that polarisation of bars at depth was difficult to achieve if the bars were corroding. On the other hand passive steel polarised relatively easily. Sagues and Kranc [6] modelled the degree of polarisation at a local anode in a galvanic cell and concluded that it may be underestimated due to activity of the macro-corrosion cells. Polder [7] used experimental methods to examine the current distribution resulting from alternative anode arrangements that were cast into reinforced concrete elements.

In a typical reinforced concrete CP system, design decisions that influence current distribution include the division of the anode system into zones, the internal resistance of the chosen anode, the location of the

* Corresponding author. Tel.: +44-207-594-5956; fax: +44-207-225-2716.

E-mail address: g.glass@ic.ac.uk (G.K. Glass).

0958-9465/02/$ - see front matter © 2002 Elsevier Science Ltd. All rights reserved.
PII: S0958-9465(01)00036-1

connections and current feeders to the anode system, the location of the current drainage point connections to the reinforcing steel and the resistance of the cables carrying the current. However, other factors associated with the steel and concrete over which the design engineer has less control will also affect current distribution.

The aim of the present work is to model the current distribution in a typical reinforced concrete CP system as a function of the condition of the steel (its corrosion rate and polarisability), the resistivity of the concrete and reinforcement geometry (bar spacing, diameter, cover depth and layers). The implication of the results on the design of a CP system will be examined.

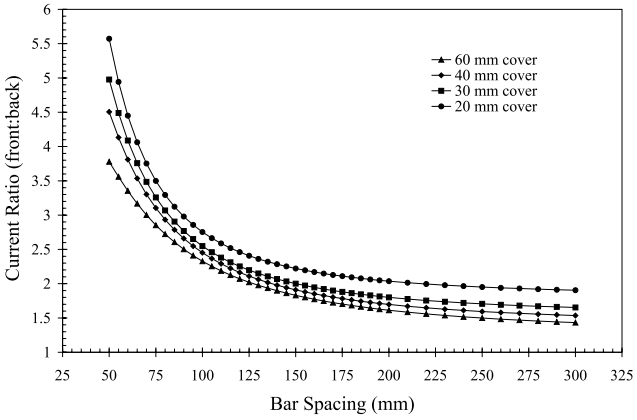

Fig. 1. The current ratio between the front and back of the central bar in equally spaced 11 bar array as a function of cover depths and bar spacings in a non-polarising boundary problem.

2. Method

2.1. Exact solution

An exact solution to the current distribution problem may be obtained for specific circumstances by applying the same theory as that used to solve electrostatic potential problems. Thus, for non-polarising interfaces, the potential distribution between an infinite planar anode and a single bar in an infinitely thick homogeneous concrete slab of uniform resistivity will be similar to that for a capacitor consisting of two parallel equidistant cylinders [8]. In this case it can be shown that the ratio of the current going to the front and back of a plain steel bar $(i_{\text{front}}/i_{\text{back}})$ of radius r placed a distance $c+r$ from the concrete surface, where c is the cover depth, is a function of the ratio of the cover depth to bar radius given by the equation:

$$i_{\text{front}}/i_{\text{back}} = 1 + 2r/c. \tag{1}$$

When there is no resistance to polarisation at the cathode and anode the current distribution is determined only by the relative geometry. The conductivity of the environment and the drive voltage will only affect the magnitude of the current.

More complicated potential distribution problems representing multiple bars may be obtained by superposition of the solution to simpler problems [8]. Thus the potential field resulting from a 11 bar array placed adjacent to an infinite planar anode is equal to the sum of the separate potential fields that would result from each bar on its own. In this case the ratio of the current between the front and back of the middle bar of 11 equally spaced 16 mm diameter bars at a fixed distance from the anode (the cover depth) is given by the curves in Fig. 1. It is evident that bar spacing and cover depth affect current distribution with an increase in bar spacing and cover depth improving current distribution.

The assumptions made, particularly that regarding a non-polarisable cathodic interface, will however render such solutions inaccurate. Only the general trends that are a function of the geometry should be extracted from such solutions. For a more accurate solution, which takes into account the boundary condition at the steel–concrete interface, numerical modelling is required.

2.2. Description of the model

For a stationary interfacial condition the current distribution is a boundary value problem. The current density vector (J) is given by a function of the form:

$$J = \frac{1}{\rho}\nabla\varphi, \tag{2}$$

where ρ is the resistivity and φ is the scalar potential field. At all points between the boundary conditions current is conserved. Thus the potential field is a solution of the Laplace equation:

$$\nabla^2\varphi = 0, \tag{3}$$

for the given boundary conditions. The problem was simplified to two dimensions by assuming that the steel reinforcement extends in the third dimension only and there is no change in the properties in this direction. In practice, however, the situation is more complicated due to the existence of transverse steel bars. Furthermore, the resistivity of concrete tends to be position-dependent as a result of carbonation and moisture gradients.

In the present work the problem was solved using a finite element model. Numerical integration in finite element calculations is usually carried out using Gaussian quadrature of the form [9]:

$$\int_{\Omega_e} f(x)\,\mathrm{d}x = \sum_{i=1}^{M} W_i f(x_i), \tag{4}$$

where W_i are the weights, x_i is the location of the points at which the integral is made, M is the total number of points and Ω_e is the element domain. The element behaviours are first expressed in terms of the functional nodal values before the final equations are then assembled for the whole structure. The potential field was thus interpolated over each element as [10]:

$$E = \sum_{i=1}^{k} E_i N_i, \tag{5}$$

where N_i is the element level interpolation function (shape function), E_i is the nodal potential value and k is the number of nodes in each element.

Using the Galerkin weighted residual method, which is the most commonly used to derive finite element equations, the weighting functions W_i in Eq. (4) are chosen to be the same as the approximating functions N_i in Eq. (5), and Eq. (3) is recast in the integral form for each element as [11]:

$$\int_{\Omega_e} N_i \nabla^2 E \, dx = -\int_{\Omega_e} \nabla N_i \nabla E \, dx + \int_{S_e} N_i \frac{\partial E}{\partial n} \, ds = 0, \tag{6}$$

where S_e is the boundary of Ω_e, s and n are co-ordinates parallel and normal to S_e. Substituting Eq. (5) into Eq. (6), the element matrix equation is obtained as [12]:

$$K^e E^e = P^e, \tag{7}$$

where

$$K_{ij}^e = \int_{\Omega_e} \nabla N_i \nabla N_j \, dx = \int_{\Omega_e} \left(\frac{\partial N_i}{\partial x} \frac{\partial N_j}{\partial x} + \frac{\partial N_i}{\partial y} \frac{\partial N_j}{\partial y} \right) dx \, dy, \tag{8}$$

and

$$P_i^e = \int_{S_e} \left(\frac{\partial E}{\partial x} n_x \frac{\partial E}{\partial y} n_y \right) N_i \, ds. \tag{9}$$

Global matrixes are assembled using the individual element matrixes to yield the global system that is then solved, subject to the boundary conditions, using a matrix inversion procedure to obtain the required nodal values [13].

2.3. Boundary conditions

At the anode, the predetermined magnitude of the current defines an average voltage gradient over the whole anode surface. The surface nodes in contact with the anode all have the same potential. It was assumed that the voltage drop through the anode material is negligible. This parameter is generally under the control of the designer. Another assumption implicit from the use of a fixed voltage gradient is that the effect of the resistance across the anode concrete interface is considered to be negligible. This will be true only if the level of anode polarisation is independent of position. While this is not usually the case, the errors resulting from this assumption may be small [6]. The use of more resistive anode materials and the interfacial resistance will be investigated in future work.

The boundary conditions at the cathode, assuming the resistance through the steel is again negligible, are provided by the polarisation conditions given by Eqs. (10)–(12) [14]. The potential shift (η) at the cathode is equal to the sum of activation (η_a) and mass transfer (η_m) effects

$$\eta = \eta_a + \eta_m. \tag{10}$$

The activation potential is defined by

$$i = i_c - i_a = i_{corr} \exp\left(\frac{2.3\eta_a}{\beta_c} \right) - i_{corr} \exp\left(-\frac{2.3\eta_a}{\beta_a} \right), \tag{11}$$

where i is the applied current, β_a and β_c are the anodic and cathodic Tafel slopes and i_{corr} is the corrosion rate. The mass transfer potential is defined by

$$\eta_m = \frac{RT}{nF} \ln\left(1 - \frac{i_c}{i_L} \right), \tag{12}$$

where i_L, R, T, n and F are the limiting current density, gas constant, absolute temperature, electronic charge number and Faraday constant, respectively. Future work will consider the spacial variation in corrosion rate on the bars and the time-dependent changes of the conditions at the steel surface [15]. In the finite element method, not applying any boundary condition on part of the domain is equivalent to applying a zero voltage gradient on that surface. This was implemented at all the other boundaries of the domain.

The boundary conditions applied in this work (potential values at the anode and current values at the cathode) are known to be of mixed Dirichlet/Neumann type [16]. Owing to the non-linear nature of the cathodic boundary conditions (Eqs. (10)–(12)), an iterative procedure was employed to achieve the analysis. This involves starting from certain values at the boundaries and changing them in steps such that the problem converges towards a unique solution. To avoid divergence a relaxation procedure was employed [17].

A 2 mm square grid was used in the finite element analysis. Convergence was shown by conservation of current i.e., current entering steel equals the current leaving anode to more than four significant figures. Typically less than 1000 iterations were needed to achieve this level of accuracy.

3. Results

3.1. A typical case

To verify the finite element analysis the model predictions were compared with previously reported results obtained using the finite difference method [18]. The applied current leaving the anode surface was set equal to 5 mA/m^2. The corrosion rate of the bars was 1 mA/m^2 which is considered to be the upper limit for passive steel [19]. Values of the cathodic Tafel slope (β_c) estimated from reported corrosion potential–corrosion rate relationships range between 120 and 230 mV [20,21]. A value of 150 mV was used in this example. A value of 300 mV was assigned to the anodic Tafel slope to represent a strongly polarised anodic reaction while the limiting current for oxygen reduction was set equal to 100 mA/m^2 [14]. The difference between the output of the finite difference and finite element analysis was typically less than 1%. This is expected as there should, in theory, be no difference between these methods for regular geometries.

An example of the results is given in Fig. 2 in which the potential distribution was computed from a planar anode to parallel 16 mm diameter bars placed at 100 mm centres with 40 mm of cover in a 150 mm thick concrete slab of resistivity 300 Ω m [9]. The resulting ratio of the current flowing to the front of the bar compared to its back was approximately 1.4. The potential shifts at the front and back of the bar were 146 and 128 mV, respectively. The results also suggest that a current of 5 mA/m^2 will induce approximately 80 mV through the concrete between the anode and the steel. It may be noted that this is sufficient to maintain a chloride concentration ratio of more than 20 between an external chloride source and the steel reinforcement [18,22]. Thus if the average external chloride concentration was 2 M, the chloride concentration at the steel would not reach 0.1 M (equivalent to about 0.4% total chloride by weight of cement) [23].

Table 1
Typical set of model input parameters

Layers of steel	1
Steel bar diameter	16 mm
Bars spacing	100 mm
Slab thickness	150 mm
Concrete cover	40 mm
Steel current density	10 mA/m^2
Anodic Tafel slope	300 mV/decade
Cathodic Tafel slope	150 mV/decade
Corrosion rate	2 mA/m^2
Oxygen limiting current density	100 mA/m^2
Anode type	Planar
Concrete resistivity	300 Ω m
Grid dimensions	2 mm

The effects of corrosion rates, anodic and cathodic Tafel slopes, oxygen limiting current density, magnitude of the applied current, resistivity of the concrete and geometry on the current and potential distribution and the voltage drop in the concrete were studied in the examples given below using the typical values of the input parameters given in Table 1 unless otherwise stated.

3.2. Interfacial condition

The effect of the corrosion rate between 0.5 and 20 mA/m^2 (approximately 0.5–20 μm/yr) on the current flowing to the front and back of the bar and on the potential shifts induced by these currents is shown in Fig. 3. An increase in the corrosion rate has a marked

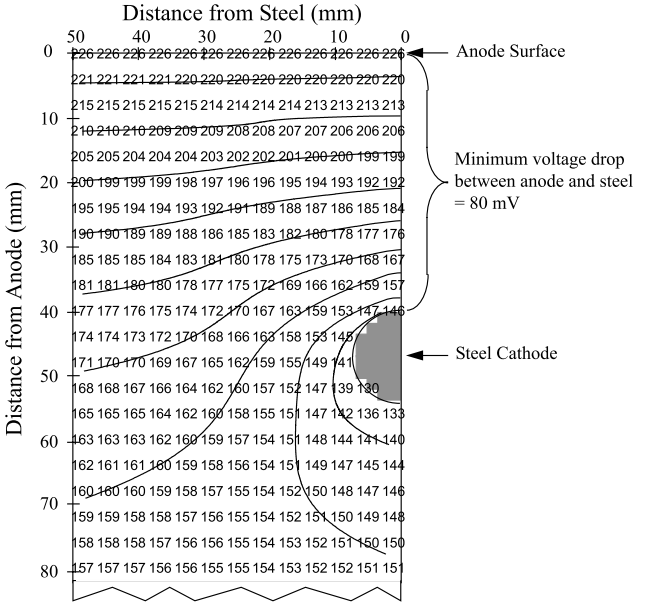

Fig. 2. Potential distribution between a planar anode and a cylindrical cathode.

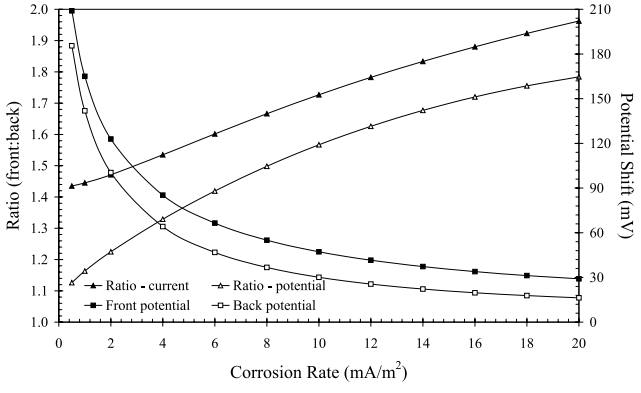

Fig. 3. Effect of the corrosion rate on current and potential distribution.

Table 2
Effect of cathodic and anodic Tafel slopes and oxygen limiting current density on current and potential distribution

Parameter	Value of parameter	Ratio of (front:back) current	Front potential shift (mV)	Back potential shift (mV)	Ratio of (front:back) potential shift
β_c (mV/decade)	60	1.87	54	39	1.37
	150	1.47	123	100	1.22
	300	1.26	230	202	1.14
β_a (mV/decade)	60	1.43	118	95	1.25
	150	1.45	120	97	1.24
	300	1.47	123	100	1.22
I_L (mA/m^2)	15	1.39	132	107	1.23
	30	1.46	125	102	1.22
	100	1.47	123	100	1.22
	180	1.47	123	100	1.22

adverse effect on both the current and potential distribution, with almost twice as much current flowing to the front of the bar than to its back at a corrosion rate of 20 mA/m^2 (cf. a ratio of about 1.4 for marginally passive steel). The potential shifts induced at the front and back of the bar were also reduced significantly with an increase in the corrosion rate. An applied current of 10 mA/m^2 induced only 15–30 mV of potential shift (back and front of the bar) when the corrosion rate was 20 mA/m^2. This may be compared with 160–200 mV induced on steel corroding at 1 mA/m^2.

The effect of the cathodic and anodic Tafel slopes and the limiting current for oxygen reduction on the current and potential distribution, when the applied current and corrosion rate of the bar were set at 10 and 2 mA/m^2, respectively, is shown in Table 2. The influence of the anodic Tafel slope and the limiting current density on both the current and potential distribution was very small. A decrease in limiting current density improved the current distribution and increased the potential shifts at the bar as its value approached the corrosion rate of the bars. An increase in the anodic Tafel slope marginally increased the potential shifts induced at the back and front of the bar. By contrast, changes in the cathodic Tafel slope strongly affected the current and potential distribution to the front and back of the bar as well as the magnitude of the potential shifts induced with more steep cathodic slopes resulting in significantly increased potential shifts as well as better current distribution around the bar.

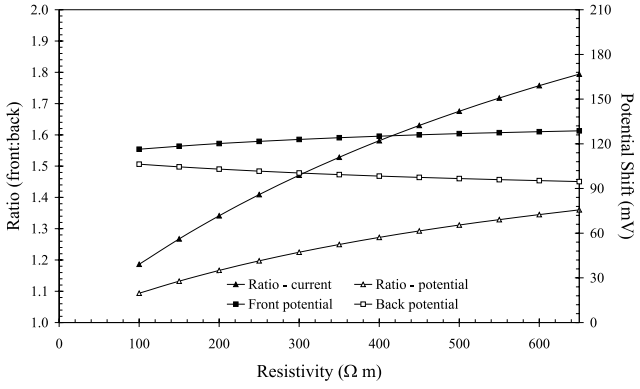

Fig. 4. Effect of the concrete resistivity on current and potential distribution.

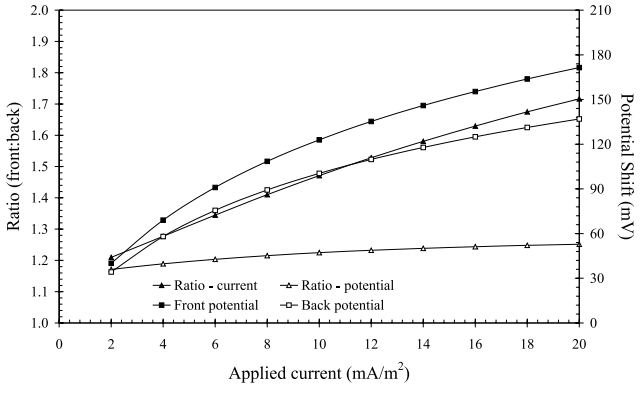

Fig. 5. Effect of the applied current on current and potential distribution.

3.3. Concrete resistivity

The effect of concrete resistivity and applied current density on the current flowing to the front and back of the bar and on the potential shifts induced by these currents is plotted in Figs. 4 and 5, respectively. The slab dimensions and parameters given in Table 1 were used as inputs to the model. Increasing both the applied current density and concrete resistivity worsened the current distribution between the front and back of the bar with the influence of the concrete resistivity being more dominant. This had an adverse effect on the potential distribution with a lower potential shift being

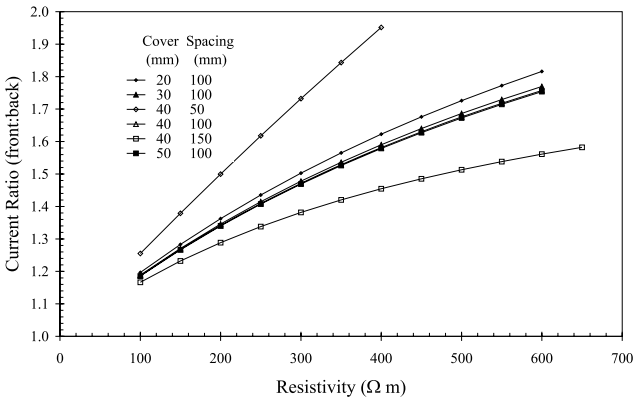

Fig. 6. Effect of concrete resistivity, bar spacing and cover depth on current distribution.

induced at the back of the bar while the potential shift at the front of the bar increased slightly.

3.4. Geometry

The effect of concrete resistivity, concrete cover and bar spacing on the current distribution is plotted in Fig. 6. An increase in the concrete cover at a given resistivity only had a limited effect on the current distribution between the back and front of the bar. By contrast, an increase in the spacing of the bars, with the anode current density kept constant, considerably improved the current distribution.

The effect of additional layers of steel at depth on the current and potential distribution is given in Table 3. Up to four equally spaced layers of parallel 16 mm diameter bars placed at 100 mm centres with concrete covers from the anode surface of 40, 88, 136 and 184 mm, respectively, in a concrete slab were examined. The ratio of current flowing to the front bar surface facing the anode compared to its back increased significantly when more than one layer of reinforcement was present at different cover depths. Thus about 3.5 times as much current went to the front bar compared to its back when four layers of steel were present in the slab compared to a ratio of about 1.5 with only one layer of steel.

The layer of reinforcement near the anode received about 70% of the total current when two or more layers of steel were present in the slab with the other 30% being distributed to the other layers. In the case of the four steel layers the ratio between the current flowing to the first bar near the anode and the last bar farthest away from the anode was as high as 14 times for a corrosion rate of 2 mA/m^2.

3.5. Voltage drop in the concrete

The effect of resistivity, concrete cover, bar spacing and corrosion rate of the bars on the voltage drop in the concrete between the steel and the anode was investigated. The effect of resistivity, concrete cover and bar spacing on the concrete voltage drop is plotted in Fig. 7. As expected increasing the cover and resistivity in-

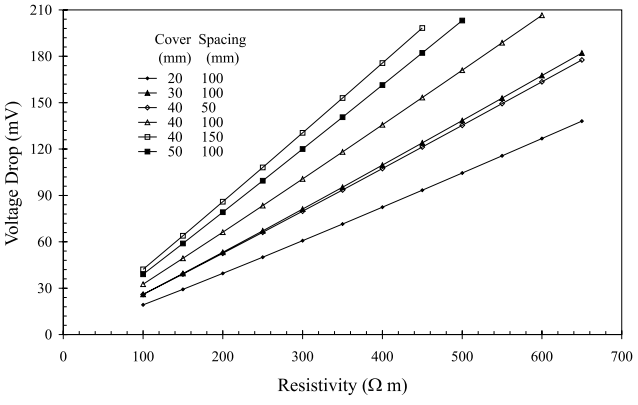

Fig. 7. Dependence of the voltage drop – resistivity relationship on bar spacing and cover depth.

Table 3
Current and potential distribution to additional layers of steel at depth

No of steel layers	Bar No.	Ratio of (front:back) current	Front potential shift (mV)	Back potential shift (mV)	Ratio of (front:back) potential shift	Ratio of (bar current:last bar current)
1	1	1.47	123	100	1.22	1.00
2	1	2.44	156	102	1.53	2.26
	2	1.24	89	78	1.15	1.00
3	1	3.03	186	116	1.61	5.76
	2	1.74	98	69	1.42	1.76
	3	1.19	61	54	1.13	1.00
4	1	3.39	209	130	1.61	13.94
	2	1.97	109	73	1.50	3.65
	3	1.56	61	44	1.40	1.59
	4	1.16	39	34	1.13	1.00

creased the voltage drop in the concrete. Increasing the spacing of the bars also increased the voltage drop in the concrete due to its dependence on the steel surface area relative to anode surface area. For example a voltage drop of 100 mV predicted for bars spaced at 100 mm with a cathode to anode area ratio of 0.64 decreased to 80 mV for bars spaced at 50 mm with a cathode to anode area ratio of 1.28 when the resistivity and cover were 300 Ω m and 40 mm, respectively. On the other hand, the effect of the bar corrosion rate on the induced voltage drop in the concrete was marginal.

4. Discussion

4.1. Uniform current distribution

The numerical results presented in this work show that uniform current distribution is difficult to achieve in reinforced concrete CP systems. For a single layer of reinforcement in typical conditions, the surface of a steel bar facing the anode may receive 1.5 times more current than the opposite surface (cf. Figs. 3–5). The current distribution is dependent on many factors. These include the resistivity of the concrete, applied current, boundary conditions describing the condition of the steel and geometry of the system.

The magnitude of the resistance to polarisation of the steel–concrete interface compared to the resistance of the concrete is an important aspect governing the current distribution [24]. If there is no resistance to polarisation at the surfaces of the anode and cathode, the current distribution will be entirely governed by the cell geometry with resistivity only affecting the magnitude of the current (Eq. (1) and Fig. 1). However, for a practical reinforced concrete CP system, both the concrete resistivity and the corrosion rate will affect the current distribution to some extent. An uneven current distribution is exacerbated when the steel is corroding and the resistance to polarisation of the steel is small compared to the resistance of the concrete. On the other hand if the steel is passive the current distribution will be more even. It may be noted that this is the case when the steel corrosion rate does not vary over the steel surface [5]. When an active passive couple exists, the current distribution will be complicated by the voltage difference between the active and passive sites [6].

The cathodic behaviour of steel in above ground concrete structures is usually under activation control [21,25]. This gives support for the use of Eq. (1) when modelling cathodic kinetics [14]. Like the corrosion rate, cathodic reaction kinetics also exert a strong influence on the polarisation of the steel. A strongly polarised cathodic reaction improves the potential and current distribution (Table 2). On the other hand the effect of the anodic reaction on the net current flowing is small when the degree of cathodic polarisation is large [26]. Thus the influence of the anodic Tafel slope is not significant. Similarly the limiting current density has little effect when the cathodic reaction rate does not approach this value.

Another factor affecting current distribution in the design of a reinforced concrete CP system is the geometry of the existing steel and concrete. The influence of this on current distribution is usually outside the control of the designer. Thus when the ratio of the installed anode to cathode area increases (when the bar to bar spacing is greater or the diameter of the steel bars is smaller) current distribution in a CP system will improve (Fig. 6). When the concrete cover to the steel is larger the current is also more uniformly distributed but its effect is limited compared to that of the anode to cathode area ratio.

4.2. Implication on drainage point connection spacing

A CP system may be viewed as an electric circuit with some of the components such as the steel and the concrete already in place. The designer has little control over the properties of these components although they also have an effect on the current distribution. As protection is commonly achieved in practice, a basis for the design of the installed components would be to ensure that any variations in current distribution arising from the installed components are small by comparison to the variations arising from the components already in place. For example, the variation in current distribution around a steel bar could be used to define the upper limit for the acceptable variation arising from the installed components.

This may be translated into acceptable voltage drops through the reinforcing steel and anode system which can then be translated into a connection spacing using Ohm's law. It is noted that there is very little discussion in the literature with respect to the principles of specifying these connection spacings for reinforced concrete CP systems. The above analysis may also be used to define the upper limit for the voltage drop through the cables carrying the current. Further work is necessary to develop guidelines to enable design decisions to be based on minimising voltage drops that affect current distribution.

4.3. Implications with regard to protection of additional layers of steel at depth

From the model predictions it is clear that in the case of CP being applied from a surface anode to multiple layers of steel, protection may be limited to the bar near to the anode, particularly when the steel is corroding (Table 3). Similar results have previously been reported

[5]. In this work the first bar near the anode received about 70% of the total current applied. This implies that for some geometries the bars farthest away from the anode may be receiving as little as 5% of the total current and thus it would not be possible to induce any voltage drop there or achieve any significant potential shift if corrosion was occurring. This will depend on the bar spacing within each layer of steel (Fig. 6). It is also noted that the back of the first layer near the anode may be screened by the other layers of steel from the protection current. Indeed the ratio between the current flowing to the front and back of the first bar was as large as 3.5 times when more than four layers of steel existed (Table 3).

The implication of these results in the design of a reinforced concrete CP system is that the first layer of reinforcement seen by the installed anode should be that which needs the protection the most. For some geometries, distributed discrete anodes may be necessary, particularly if corrosion is occurring, to maintain an adequate level of current and potential distribution. However, the spacing of discrete anodes will once again be affected by the corrosion state of the steel and further work is necessary to establish acceptable limits.

4.4. Induced protective effects

It may be noted that the factors influencing current distribution do not necessarily have the same influence on the induced negative potential shift. Thus, for example, while the effect of increasing the resistivity of the concrete on the current distribution is large, its effect on the potential shift at the steel is small (cf. Fig. 2). By contrast, a 100 mV of potential shift required by the commonly applied CP criterion [27] would be difficult to achieve if the steel was corroding (Fig. 3). It may only be achieved when the applied current is approximately five times the initial corrosion rate in conditions characterised by weakly polarised cathodic reaction kinetics [28].

It has been noted that the protective effects of a negative potential shift may not be as important in a reinforced concrete CP system as in other CP systems and may sometimes be ignored as a basis for protection [29,30]. This is because of the dominance of the inhibitive effects of an improvment in environment at the cathode that induces passivation [31]. The voltage drop induced in the concrete by the applied current provides the driving force for reducing the chloride content at the steel and maintaining a high hydroxyl concentration there, thus promoting steel passivity [32,33]. Such a voltage drop may therefore provide a basis for the choice of the cathodic protection design current density [18].

While an increase in resistivity is unfavourable in terms of current distribution (Fig. 6), it has a positive effect on the voltage drop driving the improvement in the local conditions at the steel (Fig. 7). The voltage drop is determined mainly by the applied current density and the concrete resistivity. Thus it might be necessary to increase the design current density for low resistivity concrete. However, the improving environment at the steel should be accompanied by an improvement in the current distribution and a reduction in the current requirement with time.

The numerical predictions in this work showed that an increase in the concrete cover or in the ratio of the anode area compared to the cathode area will increase the voltage drop in the concrete, with the effect being more dominant at higher resistivities (Fig. 7). This highlights an important point regarding the use of previous performance to select the design current density, namely that careful consideration should be given to differences between factors such as the concrete resistivity and geometry in the two cases as a very low concrete resistivity and cover may result in an insufficient voltage drop in the concrete.

5. Conclusions

The boundary conditions at the steel have a significant effect on current distribution with factors that increase the potential drop across the steel–concrete interface relative to the potential drop through the concrete improving the uniformity of the current distribution. Thus the current is more uniformly distributed when the corrosion rate is low as the high resistance to polarisation of interface is a controlling factor.

For a single layer of reinforcement in typical conditions, the surface of a steel bar facing the anode may receive 1.5 times the current received by the opposite surface. As CP is known to work in these cases, a basis for many design decisions that influence current distribution is that their effect is small by comparison. This may be used to define the acceptable voltage drop through the reinforcing steel and anode system which can then be translated into connection spacings and acceptable resistivities of installed components.

When more than one layer of reinforcement is present at different cover depths substantially more current may flow to the front bar surface facing the anode than to its back. Furthermore, bars farthest from the anode may receive very little of the total current. In this case the anode should be located close to the layer of steel needing the protection the most and discrete anodes may be necessary to improve current distribution.

An increase in the concrete resistivity and concrete cover and a decrease in the cathode to anode area ratio at a constant anode current density will increase the voltage drop in the concrete. These factors are important to consider in the selection of the design current

density when the principal protective effect is to generate an improvement in the environment at the steel promoting passivity.

Acknowledgements

This research was supported at Imperial College by the Engineering and Physical Sciences Research Council (grant no. GR/M02019). The authors would like to thank Mr. R. Baxter for his assistance in the experimental work. GKG is supported at Imperial College by Fosroc International Limited.

References

[1] Holser RA, Prentice G, Pond RB, Guanti RJ. Current distributions in galvanically coupled and cathodically protected tubes. Corrosion 1992;48(4):332–41.
[2] Munn RS, Devereux OF. Numerical modelling and solution of galvanic corrosion systems. Corrosion 1991;47(8):618–35.
[3] Parks AR, Thomas ED, Lucas KE. Physical scale modelling, verification with shipboard trials. Mater Perform 1991;30(5):26–34.
[4] Strømmen RD. Computer modelling of offshore cathodic protection systems: method and experience. In: Munn RS, editor. ASTM STP 1154, Computer Modelling in Corrosion. Philadelphia: ASTM; 1992. p. 229–47.
[5] Bertolini L, Bolzoni F, Cigada A, Pastore T, Pedeferri P. Cathodic protection of new and old reinforced concrete structures. Corros Sci 1993;35(5-8):1633–9.
[6] Sagüés AA, Kranc SC. On the determination of polarisation diagrams of reinforcing steel in concrete. Corrosion 1992;48(3):624–33.
[7] Polder RB. Current distribution in cathodic corrosion protection of steel in concrete, TNO Report BI-90-125, TNO Institute for Building Materials and Structures, Delft, The Netherlands; 1990.
[8] Kreyszig E. Advanced Engineering Mathematics. New York: Wiley; 1972.
[9] Press WH, Teukolsky SA, Vetterling WT, Flannery BP. Numerical recipes in FORTRAN. Cambridge: Cambridge University Press; 1992.
[10] Huebner KH, Thornton EA. The finite element method for engineers. New York: Wiley; 1982.
[11] Muralidhar K, Sundararajan T. Computational fluid flow and heat transfer. New Delhi, India: Narosa publishing house; 1995.
[12] Carvalho SLD, Telles JCF, deMiranda LRM. On the effect of some critical parameters in cathodic protection systems a numerical/experimental study. In: Munn RS, editor. ASTM 1154 Computer modelling in corrosion. Philadelphia: ASTM; 1992. p. 277–91.
[13] Cook RD. Concepts and applications of finite element analysis. New York: Wiley; 1974.
[14] Glass GK, Buenfeld NR. On the current density required to protect atmospherically exposed concrete structures. Corros Sci 1995;37(10):1643–6.
[15] Glass GK, Buenfeld NR. The inhibitive effects of electrochemical treatment applied to steel in concrete. Corros Sci 2000;42(6):923–7.
[16] Zamani NG, Porter JF, Mufti AA. A survey of computational efforts in the field of corrosion engineering. Int J Numer Meth Eng 1986;23:1295–311.
[17] Danson DJ, Warne MA. Current density/voltage calculations using boundary element techniques. In: Collected papers on cathodic protection current distribution. Houston, Tx: NACE; 1989. p. 63–79.
[18] Glass GK, Buenfeld NR. Theoretical basis for designing reinforced concrete systems. Br Corros J 1997;32(3):179–84.
[19] Gowers KR, Millard SG, Gill JS, Gill RP. Programmable linear polarisation meter for determination of corrosion rate of reinforcement in concrete structures. Br Corros J 1994;29(1):25–32.
[20] Glass GK, Chadwick JR. An investigation into the mechanisms of protection afforded by a cathodic current and the implications for advances in the field of cathodic protection. Corros Sci 1994;36(12):2193–209.
[21] Page CL, Havdahl J. Electrochemical monitoring of corrosion of steel in microsilica cement pastes. Mater Structr 1985;18(103):41–7.
[22] Glass GK, Zhang JZ, Buenfeld NR. Chloride ion barrier properties of small electric fields in the protection of steel in concrete. Corrosion 1995;51(9):721–6.
[23] Glass GK, Hassanein NM, Buenfeld NR. Neural Network Modelling of Chloride Binding. Mag Concr Res 1997;49(181):323–35.
[24] Scully JR. Polarisation resistance method for determination of instantaneous corrosion rates – critical review of corrosion science and engineering. Corrosion 2000;56(2):199–210.
[25] Glass GK, Page CL, Short NR. Factors affecting the corrosion rate of steel in carbonated mortars. Corros Sci 1991;32(12):1283–94.
[26] Stern M, Geary AL. Electrochemical polarisation: I. Theoretical analysis of the shape of the polarisation curves. J Electrochem Soc 1957;104(1):56–63.
[27] BS 7361: Part 1: 1991, Cathodic Protection–Code of Practice for Land and Marine Applications. London: British Standards Institute; 1991.
[28] Glass GK, Hassanein AM, Buenfeld NR. Monitoring the passivation of steel in concrete induced by cathodic protection. Corros Sci 1997;39(8):1451–8.
[29] Glass GK, Hassanein AM, Buenfeld NR. Cathodic protection criteria for reinforced concrete in marine exposure zones. J Mater Civil Eng 2000;12(2):164–71.
[30] Glass GK, Hassanein AM, Buenfeld NR. Cathodic protection afforded by an intermittent current applied to reinforced concrete. Corros Sci 2001;43(6):1111–31.
[31] Hassanein AM, Glass GK, Buenfeld NR. The basis for intermittent cathodic protection of reinforced concrete in the tidal zone. In: EUROCORR 2000, London: Institute of Materials; 2000.
[32] Hassanein AM, Glass GK, Buenfeld NR. Effect of intermittent cathodic protection on chloride and hydroxyl concentration profiles in reinforced concrete. Br Corros J 1999;34(4):254–61.
[33] Hassanein AM, Glass GK, Buenfeld NR. A mathematical model for electrochemical removal of chloride from concrete structures. Corrosion 1998;54(4):323–32.